Kanjirakkad. 2017. *Int. J. Turbines and Sustainable Energy*, 1(1), 8-14

doi: 10.4273/ijtse.1.1.02

International Journal of Turbines & Sustainable Energy
Available online at www.maftree.org/eja

Experimental Study of Endwall Flow in a Low-Speed Linear Compressor Cascade: Effect of Over-tip Leakage

Vasudevan Kanjirakkad

Thermo-Fluid Mechanics Research Centre, University of Sussex, United Kingdom

ABSTRACT:

This paper describes the study of endwall flow modification due to over-tip leakage flow in axial compressor blades. Un-shrouded axial compressor stator and rotor blades in aero-engines and land based gas turbines are subjected to over-tip leakage flow to allow for the relative motion between the unsupported end of the aerofoil and the near endwall surface that moves relative to it. The leakage flow that results is unturned by the blade and this causes non-uniform flow downstream of the blade-row that mixes out to produce a total pressure loss. The leakage flow also causes the formation of a 'leakage-vortex' which causes further losses within and downstream of the blade-row through its own viscous mixing with the fluid around it. In many compressors the blockage created by these effects is known to dictate the point of stall inception and hence the stability of the compressor and its useful operating range. In this paper an experimental study into the effects of the leakage flow, namely, the formation of the leakage vortex and the generation of the losses under a low Reynolds number condition is discussed. It has been shown that the endwall flow is significantly altered by the presence of the leakage vortex as it weakens the classical secondary flow.

KEYWORDS:

Compressor; Cascade; Leakage; Loss

CITATION:

V. Kanjirakkad. 2017. Experimental Study of Endwall Flow in a Low-Speed Linear Compressor Cascade: Effect of Over-tip Leakage, *Int. J. Turbines & Sustainable Energy*, 1(1), 8-14. doi:10.4273/ijtse.1.1.02.

NOMENCLATURE & ABBREVIATIONS

C	Blade chord (mm)
Lx	Pitchwise distance from blade suction side
Ly	Spanwise distance from nearest endwall
P	Pressure (Pa)
Re	Reynolds number (chord based)
Y_p	Total pressure loss coefficient
h	Blade height (mm)
s	Blade pitch (mm)
α, β	Flow angle and Blade angle (degrees)
δ	Boundary layer thickness (mm)
χ	Stagger angle
$*_1$, $*_2$	Cascade inlet and exit static conditions
$*_{01}$, $*_{02}$	Cascade inlet and exit total conditions
PS	Blade pressure side
SS	Blade suction side
t/c	Tip clearance gap (% of span)

1. Introduction

The over-tip leakage is the inevitable result of the need to maintain relative motion between the unsupported end of the blade and the endwall. Un-shrouded stator and rotor compressor blades in aero-engines and land based gas turbines are affected by this. In the case of cantilevered stator blades this results in what is known as the 'hub-leakage flow' and in the case of plain tip rotor blades this would be called the 'tip-leakage flow'. In either case the leakage flow that results is unturned by the blade and this causes non uniform flow downstream of the blade-row that mixes out to produce a total pressure loss. Some of this leakage flow also rolls-up into a 'leakage-vortex' which produces further losses within and downstream of the blade-row as it interacts with the fluid around it. Considerable blockage is created by the presence of the leakage fluid and the vortex and it is known that stall inception and compressor operating range could be dictated by these features. The over-tip leakage flow in axial flow compressor blade-rows has been a major topic of research over the years.

The effect of leakage and secondary flows in a low-speed linear compressor cascade was described by Lakshminarayana and Horlock [1]. Their experimental study revealed that leakage and the secondary flow effects could counter-act and reduce the adverse effects of one-another. Hunter and Cumpsty [2] experimentally studied the effect of inlet boundary layer across an isolated compressor rotor. The boundary layer skew has been stated to introduce streamwise vorticity directing the fluid towards the pressure side of the blade passage and the development of the boundary layer was shown to be severely affected by the tip clearance flow. Inoue et al [3] used multi-sample ensemble averaged phase locked data to study the tip leakage flow downstream of an isolated compressor rotor. They reported the existence of an inflexion point in flow angle at blade exit as a result of the vortex roll up. At larger tip gaps the vortex core was found to move tangentially away from the blade suction side. Inoue and Kuroumaru [4] studied, in detail, the structure of the leakage vortex using a similar set-up as Inoue et al [3]. They noticed that as the tip gap is increased the location of maximum pressure difference

across the tip, and hence the onset of the vortex roll-up moved downstream thus producing a stronger vortex behind the blade. The trajectory of the vortex was found to be aligned with the trough of the wall static pressure measured over the endwall. Storer and Cumpsty [5] reported experimental study in a linear cascade with tip clearance and complemented it with a numerical study. They found the tip leakage flow to separate over the tip surface near the pressure side corner and then remain separated over a majority of the chord. They concluded that the tip leakage flow, which is primarily inviscid, is strongly related to the blade loading.

Chen et al [6] carried out a similarity modelling of the cross passage flow in the clearance region using the slender body approach. The study focussing on the structure of the clearance vortex predicted the trajectory of the tip clearance vortex using only the mean blade flow angles and the blade camber line as input. Apart from reinforcing the inviscid nature of the leakage mechanism their analysis predicted that the vortex trajectory is independent of the gap and that its centroid remains at a constant radial height downstream of the blade trailing edge. In the continuing discussion following this paper Storer described the effect of skewed inlet boundary layer in rotating machines (as opposed to collateral boundary layers that are present in linear cascades with no relative wall motion). It is pointed out that the effect of the inlet skew is to increase the incidence near the tip which in turn brings the location of peak suction closer to the leading edge and the onset of the leakage vortex along with it.

The IGTI scholar lecture on loss mechanisms by Denton [7] drew the distinction between the loss of work due to leakage (which is reversible) and the entropy generation that results in irreversible loss. An approximate method to estimate the leakage loss was also proposed by the above author. Kang and Hirsch [8] noticed the existence of a tip separation vortex at the tip gap entrance from about the mid-chord as the leakage flow diverges above the tip surface and accelerates over it. This vortex was found to gain in strength along the chord. A numerical study by the same authors [9] of the linear compressor cascade (that was used in the previous study) also investigated the effect of relative motion of the endwall. It was noted that at high flow coefficients with relatively lower wall entrain-ment the leakage vortex is shifted towards the suction surface. The discussion that follows at the end of this paper (Cumpsty and Greitzer) is very lively and sheds more light into the effects of relative wall motion and inlet boundary layer skew as present in a real compressor rotor. Gbadebo et al [10] investigated tip clearance in a compressor cascade and noted that above 0.58% clearance (based on chord) the 3-D separation and the corner vortex reduced considerably due to the suppression of the horse-shoe vortex. The separation lines due to the endwall flow are shown to be replaced with new 3-D separation lines that are linked to the leakage vortex.

In the present study aerodynamic measurements are conducted in a low speed linear cascade facility. The objective is to understand the modification of the endwall flow due to the over-tip leakage flow and the vortex that is generated. Throughout testing an inlet velocity of 20 m/s was used and this corresponded to a chord based Reynolds number of approximately 110,000. This is relatively low even for the rear stages of present day aero engine compressors under cruise conditions. However these con-ditions could still exist during off-design operations such as start-up or hot-restarts in the event of emergency en-gine shut off in mid-air. In the future there is potential demand for the design of smaller and efficient engines for low noise podded engine aircrafts and land based gas turbines for distributed power generation. Compressors with very low radii are therefore required and low Reynolds number operation would become inevitable especially in the rear stages. The loss generation and leakage vortex interaction are looked at corresponding to 1%, 2% and 3% tip gaps with respect to the blade span.

2. Experimental methodology

The experiments are conducted in a low-speed linear cascade consisting of three blades and four passages. The blade shapes are based on the NACA65 family of vanes used in the University of Darmstadt axial compressor test rig. The 2-D profile used here is extracted from that at 10% span of the above vane. Albeit the use of only three blades, the cascade used here is a scaled version of the geometry used in the study by Meyer et al [11]. A sketch of the cascade arrangement is shown in Fig. 1. The airflow is sourced from a screw type rotary compressor. Prior to reaching the test section the air goes through a drier and a settling chamber. Since the ducting includes an unavoidable elbow bend a series of gauzes are installed downstream of the elbow bend to make the flow uniform at the inlet to the cascade. A combination of four pitot-tubes and static pressure taps installed at 5 blade-chords upstream of the cascade inlet measures the inlet flow conditions.

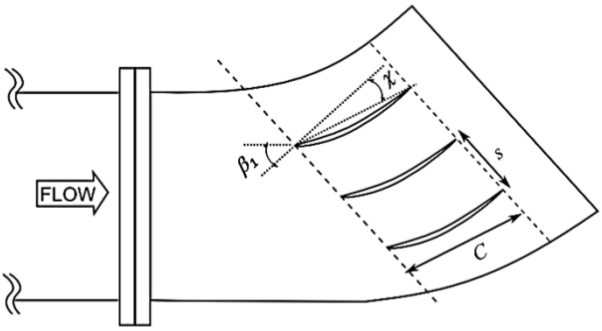

Fig. 1: Linear compressor cascade arrangement

A calibrated 3-hole probe is traversed at a distance of 70% blade-chord downstream of the aerofoil trailing edge to survey the blade exit flow field. A traverse gear with three axes of freedom is used for this purpose. The linear cascade geometric parameters and test flow conditions are summarised in Table 1. Despite the use of only three blades an acceptable level of flow periodicity is achieved as seen from the total pressure coefficient (see Eqn. (1)) distribution at the cascade exit in Fig. 2. The central blade is used for detailed measurement as presented in the rest of this paper. The tip gap is only varied over this central blade. The different tip gaps are achieved by the use of an endwall cassette through

which the aerofoil can slide in and out of the cascade and could also be locked in position. The tip gap is then accurately set using feeler gauges. No tip gap is present on the other blades on either side of the central blade.

Table 1: Cascade parameters and test flow conditions

Parameter	Value
Blade chord, *C*	80 mm
Blade pitch, *s*	44 mm
Blade aspect ratio, (*h*/*C*)	1
Inlet blade angle, β_1	42°
Stagger angle, χ	15.2°
Inlet flow velocity, V_1	20 m/s
Reynolds number, *Re*	106667
Inlet boundary layer thickness, δ	6 mm

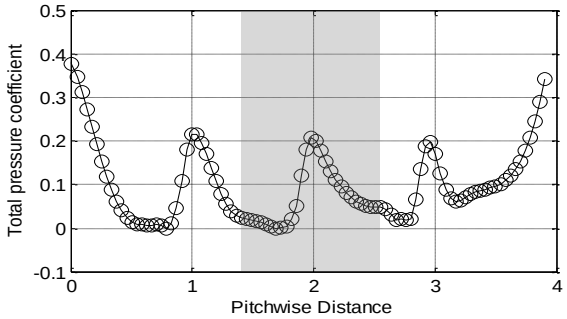

Fig. 2: Total pressure coefficient at mid-height across the cascade exit (the shaded region marks the test blade)

3. Results and Discussion

The results from 3-hole probe area traverses conducted at a distance of 70% blade-chord downstream of the aerofoil trailing edge are presented in this section. The flow periodicity of the cascade was first established by carrying out a pitchwise line traverse at mid-height along the whole exit of the cascade and the result was already presented in Fig. 2. The detailed area traverses are only conducted downstream of the middle blade. The pitchwise extent of the traverse is one blade-pitch and the spanwise extent is from the near endwall where the tip gap is set to the blade mid-height. The traverse grid consists of 20 spanwise positions and 25 pitchwise positions both having non-uniform grid spacing. The total pressure loss between the inlet and the exit of the cascade is presented as a loss coefficient defined as:

$$Y_p = (P_{01} - P_{02})/(P_{01} - P_1) \quad (1)$$

Here P_{01} and P_1 refer to the average inlet total pressure and static pressure, respectively, measured using the pitot-tubes and static tappings installed in the inlet duct as described earlier in the paper. P_{02} is the measured total pressure at the cascade exit using the 3-hole probe.

The total pressure loss coefficient (Y_p) contours at the cascade exit for the three different tip gaps tested and for the datum case with no gap are shown in Fig. 3. Although the tip leakage vortex generation is known to be an inviscid process (pressure driven) the subsequent mixing of this vortex with the flow downstream is not. A larger tip gap can be seen to produce a larger vortex and this in turn produces a larger loss-core or region of total pressure deficiency. In the datum test case with no tip gap, a loss-core due to the secondary flow is visible centred around 25% span. The secondary vortex which has a clockwise sense is located at around 8% span and this is more discernable from the contours of flow angle (α) presented in Fig. 4. As the tip gap is opened up the loss-core due to the secondary flow and the associated vortex is no longer visible and the latter is suppressed by the leakage vortex as can be seen from the total pressure contours for the 1% tip gap case in Fig. 3 and the corresponding flow angle contours in Fig. 4. Instead a large loss-core extending from the endwall to about 25% span and centred at around 10% span is present. The leakage vortex core is located slightly below at about 5% span as seen from the flow angle contours. The leakage vortex is much bigger than the secondary vortex that existed in the datum case and notably is in the opposite sense (anti-clockwise) therefore negating the former. The opposite sense of these two vortices has been discussed by Lakshminarayana and Horlock [1]. The endwall boundary layer that is visible in the datum case is swept away by the presence of the leakage vortex. As the tip gap is increased to 2% and subsequently to 3%, the general nature of the secondary flow remains the same as in the 1% case, however the loss-core and the vortex core increase in size.

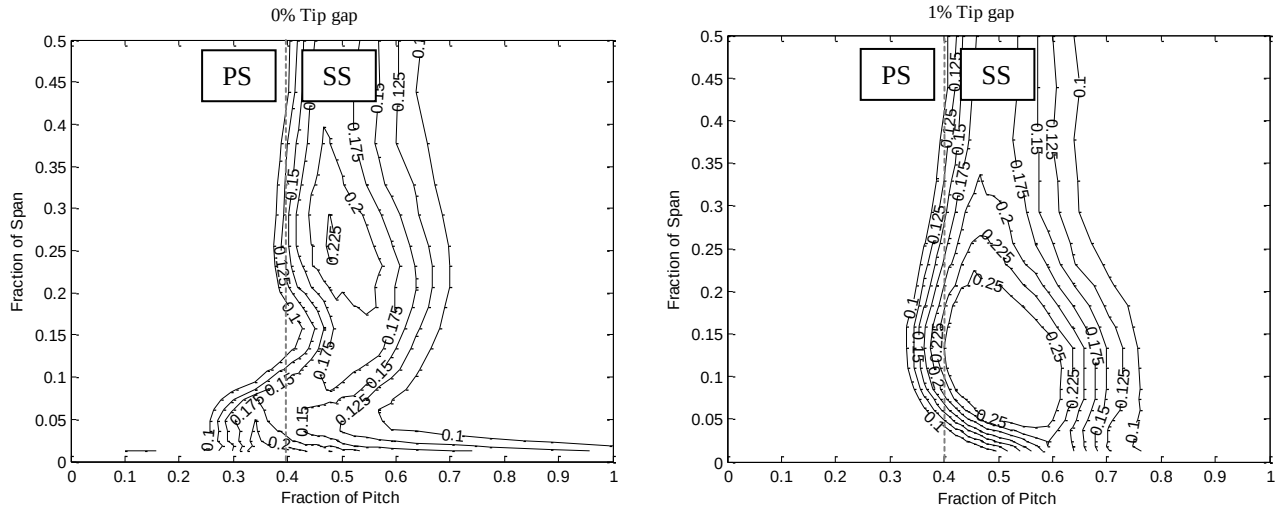

Fig. 3(contd.): Contours of total pressure loss coefficient for different tip gaps at cascade exit (70% blade-chord from trailing edge)

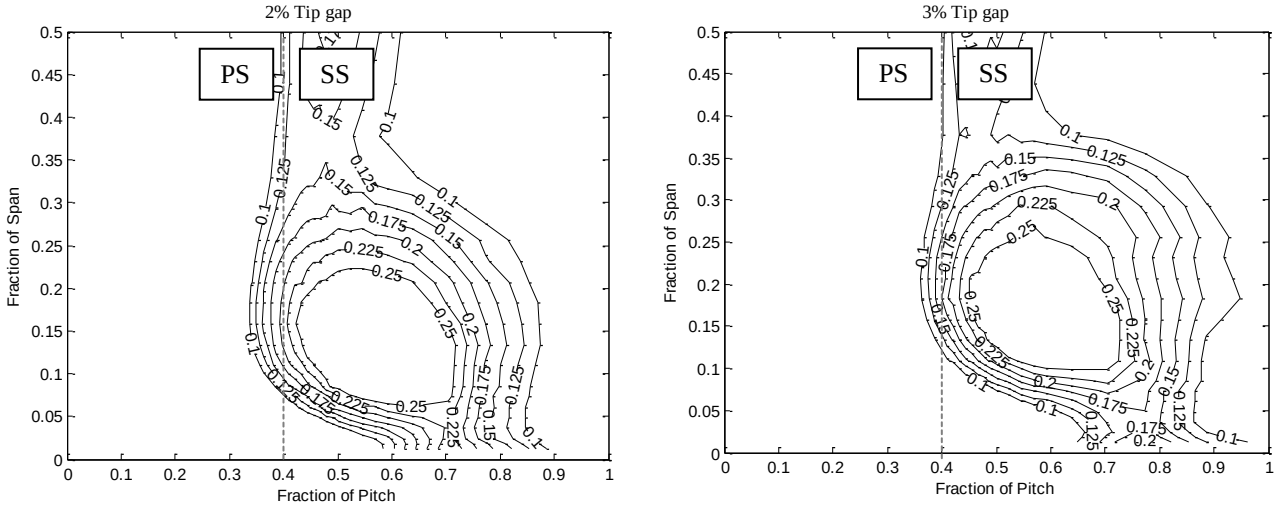

Fig. 3: Contours of total pressure loss coefficient for different tip gaps at cascade exit (70% blade-chord from trailing edge)

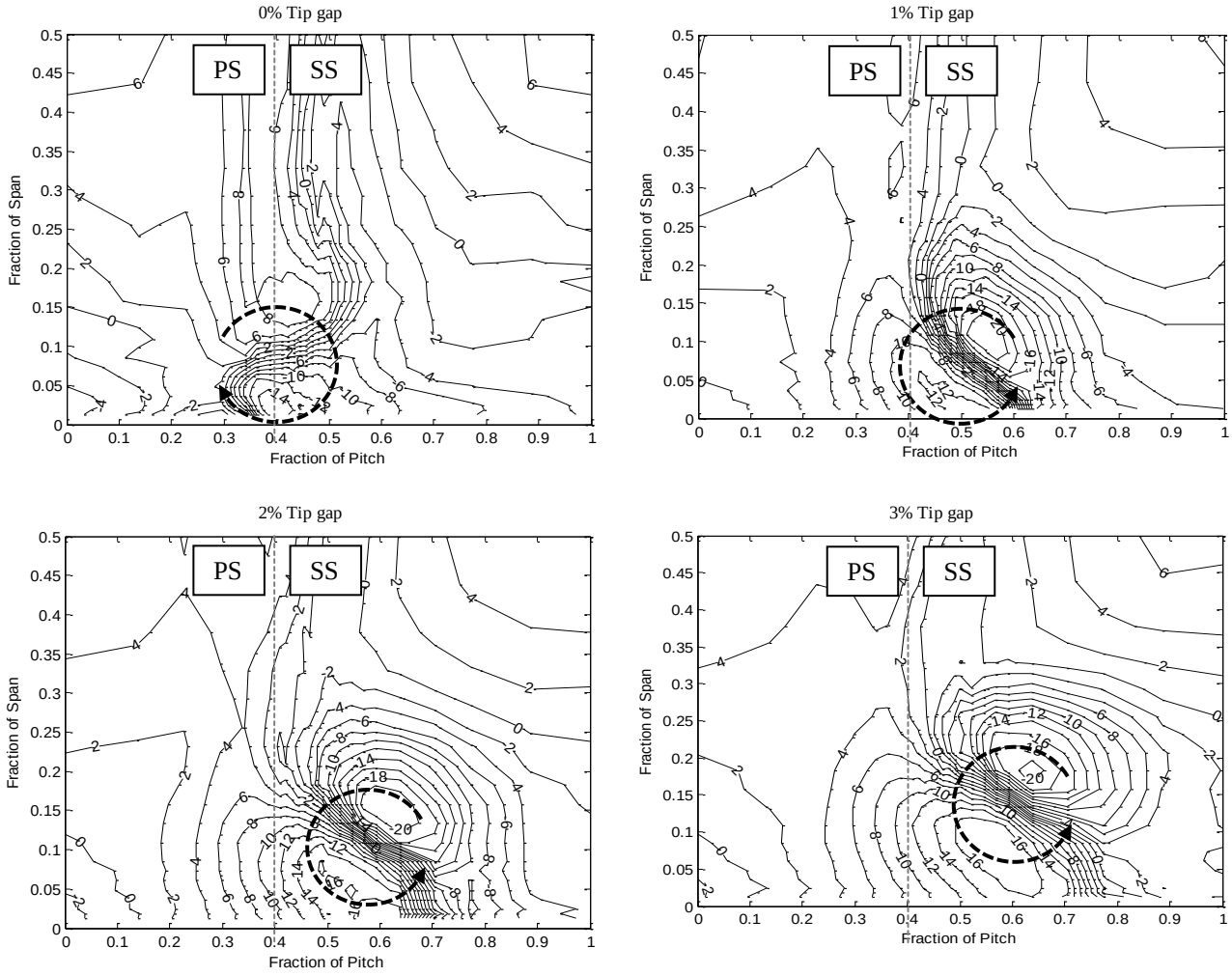

Fig. 4: Contours of flow angle for different tip gaps at cascade exit (70% blade-chord from trailing edge)

An increase in vortex strength at larger tip gaps was previously observed by others including Inoue et al [3]. Both the loss-core and the leakage vortex core migrate away from the endwall with increasing tip gap but it is interesting that they move. closer to each other when leakage is present with a stronger and larger vortex resulting in increased proximity. At higher gaps as the leakage vortex moves outwards, the endwall boundary layer slowly re-establishes as seen from the loss contours for the 3% tip gap case. A pitchwise movement of the vortex core is also visible from the flow angle contours. This finding disagrees with the simplified similarity model proposed by Chen et al [6] whose model for leakage vortex trajectory estimates the vortex core location to be independent of the tip gap at a given radius. This fixes the tangential position of the core in relation to the suction surface at a given axial distance. However, a pitchwise movement of the vortex core is supported by the findings of Inoue et al [3] and Inoue and Kuroumaru[4].

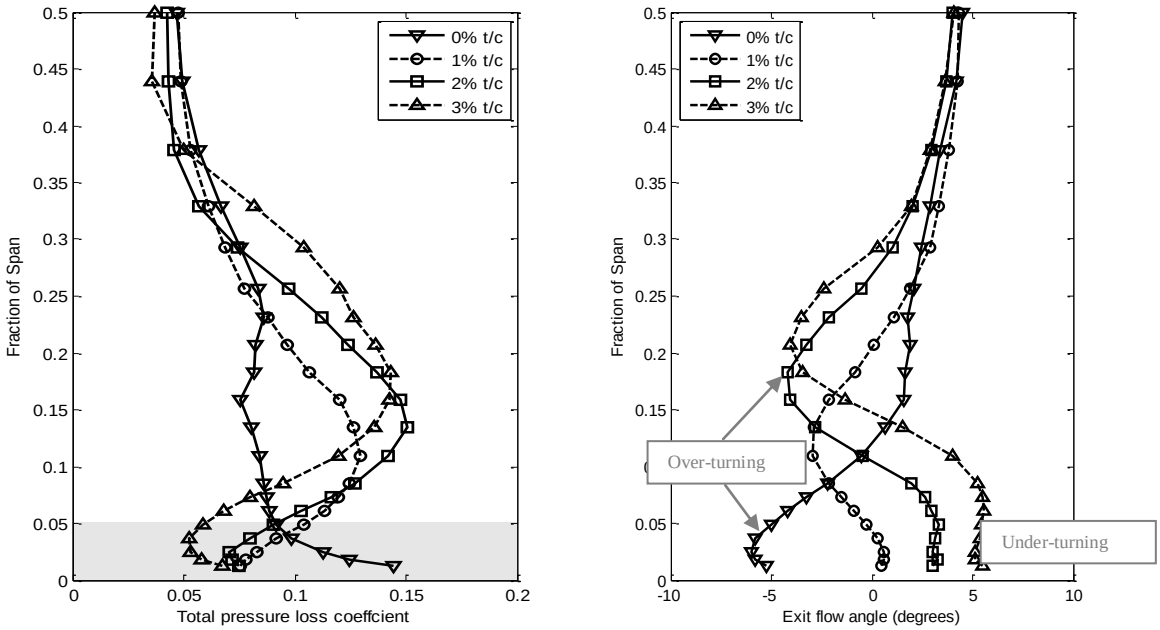

Fig. 5: Spanwise distribution of pitchwise area averaged total pressure loss coefficient and flow angle at cascade exit (the shaded region represent the inner 5% of span over which the near-wall loss is estimated)

The spanwise distribution of the pitch-wise mass averaged total pressure loss coefficient (Eqn. 1) and the circumferential flow angle are presented in Fig. 5 for the datum (no-gap) case and the three tip gap cases that were tested. It would be convenient to look at the distribution if we split the measured spanwise extent (0-50% of span) into a near-wall region (0-5% of span as shown by the shaded region in Fig. 5) and an outer region (5-50%) span where clear trends are visible. In the near-wall region the highest losses occur for the no-gap case for which there exists a well-defined endwall boundary layer region as seen in loss-coefficient contour plots in Fig. 3. As the tip gap is opened up and the endwall boundary layer is swept away by the leakage vortex the loss-coefficient gradually reduces. The lowest loss in the near-wall region is observed for the largest of the three tip gaps tested (3%). It is also seen that near the endwall the loss is lower for the 1% tip gap case compared to the datum. Interestingly, as the tip gap is increased further the tip vortex core forms away from the endwall and this results in the slow re-establishment of the endwall boundary layer below the loss/vortex core as we noted previously in Fig. 3. This has the visible effect of an increased loss (forward bent of the curve) very close to the endwall as seen in the radial distribution of loss for the 2% and 3% tip gap case in Fig. 5.

In the outer region (5-50% of span), where the tip clearance vortex core is present, the peak value and the spanwise extent of the loss is seen to scale with the tip gap size. The peak value associated with the loss-core is observed to migrate away from the endwall as tip gap is increased, however, the maximum value of the peak is observed at 2% tip gap and not for the highest tip gap tested (3%). The spanwise extent of the loss-core is marginally larger for the 3% tip gap case. This produces a slightly higher loss overall. The spanwise distribution of pitch-averaged flow angle (α) also shows very distinctive profiles for the cases tested. For the datum no-gap case the most notable feature is the classical overturning associated with the secondary flow near the endwall. As the tip gap is introduced an inflexional profile starts to appear as noted by Inoue et al [3]. The point of inflexion is approximately centred on the averaged vortex. As clearly seen from Fig. 5 the effect of the inflexion is to produce under-turning near the end wall (and hence negate the endwall secondary flow) and overturning further up the span on the other side of the vortex. Clearly, the larger the tip gap is larger is the inflectional region, both in terms of the magnitude of flow angle change and in the spanwise extent of it. Inflexional profiles are also seen in the study by Hunter and Cumpsty [2] who measured the relative flow angles downstream of a low-speed compressor rotor at different tip clearances. In the above study, the degree of inflexion diminishes as the flow coefficient is lowered as it changes the tip loading and hence the relative strength of the tip vortex.

Mass averaged quantities over the area-traversed region (0 to 50% of span and over 1 blade pitch) are presented next. The change in total pressure loss coefficient values is presented first for the various tip gap cases in Fig. 6. Loss values split between the inner 5% (the shaded region in Fig. 5) of span and the outer region (5 to 50% of span) are also shown. As expected, the overall loss measured over the 50% span is the lowest when there is no tip gap present as indicated by the total pressure loss coefficient values. About 10% rise in the value of the loss coefficient is observed when the 1% tip gap is introduced with respect to the datum case. A similar but slightly smaller rise is seen when the gap is increased from 1% to 2%. However no significant increase in loss is seen as the gap is increased from 2 to 3%. On comparing the mass weighted loss coefficient values for the inner (0-5%) and the outer (5-50%) regions, also shown in Fig. 6, it is clear that as the loss grows with tip size in the outer region the opposite happens in the inner region. The loss in the inner region that contributed significantly (in a mass weighted sense)

to the overall loss is greatly reduced as the vortex core moves away from the endwall. So the reduced loss in the near-wall region is responsible for the slow-down in the growth of loss that was noted above.

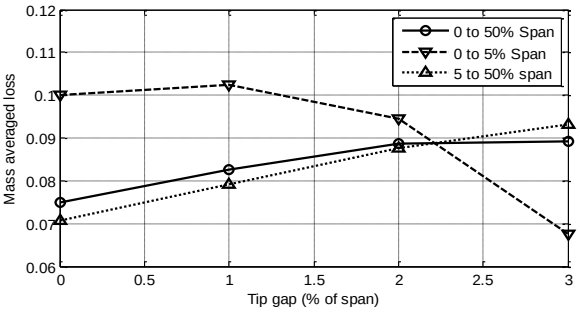

Fig. 6: Mass averaged loss calculated over 50% spanl

The relative positions of the loss-core as identified from the total pressure loss coefficient contours shown in Fig. 3 and the leakage vortex core as identified (albeit approximately) from the flow angle contours presented in Fig. 4 are discussed next. The conventions and the symbols used to locate the coordinates are sketched in Fig. 7. Pitchwise distance of the vortex core (L_{xv}) and the loss-core (L_{xl}) are measured from the dotted line representing the trailing edge in Figs. 3 and 4, which by definition also represents the suction surface at this axial location. Spanwise distance of the vortex core (L_{yv}) and the loss-core (L_{yl}) are measured from the nearest endwall.

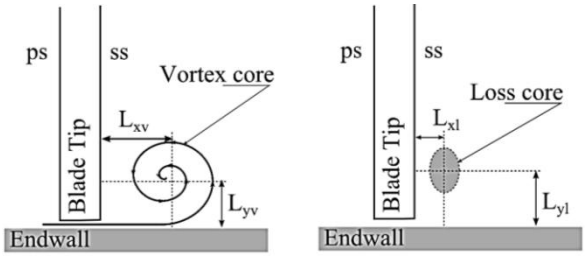

Fig. 7: Cartoon showing the description of the location of loss-core and the vortex on the measurement plane

The spanwise and the pitchwise migration of the loss-core and the vortex core as the tip gap is varied is presented in Fig. 8 and Fig. 9 respectively. In the datum case with no tip gap a secondary flow vortex is present and the vortex core and the loss-core are well separated from each other by over 15% of span and nearly 10% of the blade pitch. For all cases, invariably, the loss-core is located at a simi-lar or higher spanwise location compared to the vortex core. As it was also noted by Inoue et al [3], the vortex moves away from the blade suction surface as the tip clearance is increased. As the tip leakage is introduced and a leakage vortex is formed the spanwise separation between the loss-core and the vortex core (in this case the leakage vortex) is reduced to within 5% of span and they are almost co-located in the pitchwise sense. This is, however, easily explained since the tip leakage weakens the effect of the secondary flow and the major loss producing feature is also associated with the core of the leakage vortex. The uncertainty in the measurement of flow angle is better than 0.5° and that in determining the values of the pressure coefficients only better than 0.005. Although the trends presented here are likely to be true and hence back up the physical explanations that are provided, the exact values presented should be taken in this context.

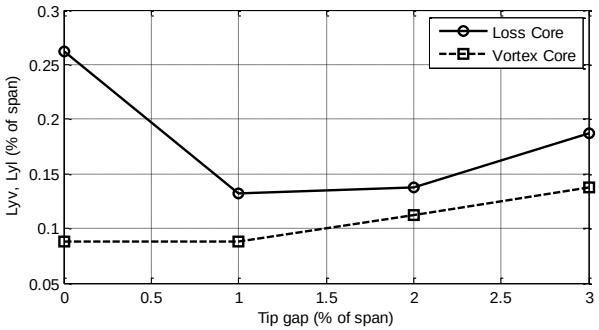

Fig. 8: Spanwise location of the loss-core and vortex core measured from the nearest

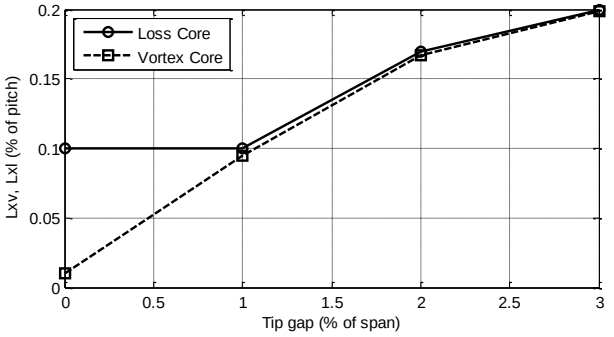

Fig. 9: Pitchwise location of the loss-core and vortex core measured from the blade suction surface at trailing edge

4. Conclusion

Experiments have been carried out at a low Reynolds number inside a simple linear compressor cascade to understand the effect of blade tip clearance on the formation of the leakage vortex and the endwall/secondary flow. Three different tip clearances (1%, 2% and 3% of span) were tested and results compared with that from a datum case with no tip gap. The following conclusions were drawn from the study:

- A distinct loss-core and secondary vortex are present in the datum case with no tip gap.
- The introduction of the 1% tip gap and the higher gaps resulted in the formation of a leakage vortex that dominates the near-wall flow.
- The leakage vortex has an opposite sense compared to the classical secondary flow vortex and therefore negates the effects of the latter.
- The effect of the leakage vortex is to weaken the secondary flow and remove the overturned endwall boundary layer.
- The loss associated with the inner 5% of span near the wall is significantly higher for the no-gap and low tip gap cases but this reduces rapidly as the tip gap is increased.
- An inflexional nature is observed in the spanwise distribution of the circumferential flow angle centred around the core of the leakage vortex.
- The spanwise and pitchwise proximity of the loss-core and the vortex is greatly increased with the increase in tip gap and the associated vortex strength.

ACKNOWLEDGEMENTS:

The work described in this paper is a result of multiple student projects supervised by the author at the University of Sussex. The author would wish to thank the Department of Engineering and Design at Sussex for funding the experiment hardware through projects. More importantly thanks are due to the project students; Jonathan, Glen, Omar and Laurence who took part in the hardware design/set-up and the testing at various stages. The author would also like to thank Meyer et al [11] for providing with the coordinates of the aerofoil.

REFERENCES:

[1] B. Lakshminarayana and J.H. Horlock. 1967. *Leakage and Secondary Flow in Compressor Cascades*, ARC Report and Memoranda No 3483.

[2] I.H. Hunter and N.A. Cumpsty. 1982. Casing wall boundary-layer development through an isolated compressor rotor, *ASME J. Engineering for Power*, 104, 805-817. http://dx.doi.org/10.1115/1.3227347.

[3] M. Inoue, M. Kuroumaru and M. Fukuhara. 1986. Behavior of tip leakage flow behind an axial compressor rotor, *ASME J. Engineering for Gas Turbines and Power*, 108, 7-13. http://dx.doi.org/10.1115/1.3239889.

[4] M. Inoue and M. Kuroumaru. 1989. Structure of tip clearance flow in an isolated axial compressor rotor, *ASME J. Turbomachinery*, 111, 250-256. http://dx.doi.org/10.1115/1.3262263.

[5] J. A. Storer and N.A. Cumpsty. 1991. Tip leakage flow in axial compressors, *ASME J. Turbomachinery*, 113(2), 252-259. http://dx.doi.org/10.1115/1.2929095.

[6] G.T. Chen, E.M. Greitzer, C.S. Tan and F.E. Marble. 1991. Similarity analysis of compressor tip clearance flow structure, *ASME J. Turbomachinery*, 113(2), 260-271. http://dx.doi.org/10.1115/1.2929098.

[7] J. Denton. 1993. Loss mechanisms in turbomachines, *ASME J. Turbomachinery*, 115(4), 621-656. http://dx.doi.org/10.1115/1.2929299.

[8] S. Kang and C. Hirsch. 1994. Tip leakage flow in linear compressor, *ASME J. Turbomachinery*, 116(4), 657-664. http://dx.doi.org/10.1115/1.2929458.

[9] S. Kang and C. Hirsch. 1996. Numerical simulation of three-dimensional viscous flow in a linear compressor cascade with tip clearance, *ASME J. Turbomachinery*, 118, 492-502. http://dx.doi.org/10.1115/1.2836694.

[10] S.A. Gbadebo and N.A. Cumpsty, T.P. Hynes. 2007. Interaction of tip clearance flow and three-dimensional separations in axial compressors, *ASME J. Turbomachinery*, 129(4), 679-685. http://dx.doi.org/10.1115/1.2720876.

[11] R. Meyer, S. Schulz and K. Liesner, H. Passrucker, R. Wunderer. 2012. A Parameter study on the influence of fillets on the compressor cascade performance, *J. Theoretical and Applied Mechanics*, 50(1), 131-145.